20/2019

Cover Feature:
M.-S. Park et al.
Thermoplastic Polyurethane Elastomer-Based Gel Polymer Electrolytes
for Sodium-Metal Cells with Enhanced Cycling Performance

A Journal of

ChemPubSoc
Europe

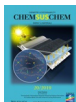# Thermoplastic Polyurethane Elastomer-Based Gel Polymer Electrolytes for Sodium-Metal Cells with Enhanced Cycling Performance

Myung-Soo Park,[a] Hyun-Sik Woo,[a] Jung-Moo Heo,[a] Jong-Man Kim,[a] Ranjith Thangavel,[b] Yun-Sung Lee,[b] and Dong-Won Kim*[a]

Sodium batteries have been recognized as a promising alternative to lithium-ion batteries. However, the liquid electrolyte used in these batteries has inherent safety problems. Polymer electrolytes have been considered as safer and more reliable electrolyte systems for rechargeable batteries. Herein, a thermoplastic polyurethane elastomer-based gel polymer electrolyte with high ionic conductivity and high elasticity was reported. It had an ambient-temperature ionic conductivity of $1.5\ mS\,cm^{-1}$ and high stretchability, capable of withstanding 610% strain. Coordination between Na^+ ions and polymer chains increased the degree of salt dissociation in the gel polymer electrolyte compared with the liquid electrolyte. An Na/ $Na_3V_2(PO_4)_3$ cell assembled with gel polymer electrolyte exhibited good cycling performance in terms of discharge capacity, cycling stability, and rate capability, which was owing to the effective trapping ability of organic solvents in the polymer matrix and uniform flux of sodium ions through the gel polymer electrolyte.

Introduction

The amount of fossil fuels is limited and the demand for efficient energy management systems increases, and consequently considerable research is being conducted on green renewable energy sources and energy-storage systems. After the lithium-ion battery (LIB) was commercialized by Sony Corporation in 1991, it has been a leading battery technology used for various applications, such as portable electronic devices, electric vehicles, and large-scale energy-storage systems, owing to its high energy density and long cycle life.[1] However, increasing market demand for lithium and limited lithium resources have resulted in a rise in battery costs.[2] Thus, sodium-based batteries are a promising alternative to LIBs because of the natural abundance of sodium and low cost of sodium resources.[2b,c] Furthermore, many characterization methods and synthetic strategies currently used for materials in LIBs can be also utilized for their sodium counterparts because they share similar alkali-metal ion chemistry.[3]

To date, a variety of electrode materials have been extensively investigated for sodium batteries with liquid electrolytes and commercial separators.[4] The electrochemical performance of the electrode materials has gradually improved owing to the efforts of many researchers. However, like LIBs, liquid electrolytes composed of organic solvents and inorganic salt cause inherent safety problems owing to the high flammability of the organic solvents.[5] To address the safety issues caused by liquid electrolytes, polymer electrolytes have received considerable attention for battery applications. Solid polymer electrolytes based on poly(ethylene oxide) have been actively explored; however, their low ionic conductivities at room temperature preclude their use in batteries.[6] In contrast, gel polymer electrolytes that have high ionic mobility in the liquid phase and can be prepared as a thin flexible film have several advantages, such as high ionic conductivity, good interfacial adhesion to electrodes, and suppression of solvent leakage.[7] Numerous polymer materials, including poly(vinylidene fluoride-*co*-hexafluoropropylene), polyacrylonitrile, poly(methyl methacrylate), polydopamine, and poly(ethylene glycol) methyl ether methacrylate, have been utilized in preparing gel polymer electrolytes for sodium-battery applications.[5b,7c,8] Thermoplastic polyurethane (PU) elastomer is a linear segmented block copolymer composed of hard and soft segments, which thus exhibits a phase-separation morphology owing to the immiscibility of the hard and soft segments.[9] The phase separation leads to the formation of hard-segment domains derived from strong intermolecular hydrogen bonding and a flexible soft-segment matrix. The hard-segment domains function as physical cross-links to the soft-segment matrix, and this results in high elasticity. The soft-segment domains endow PU with flexible and stretchable properties, and it can dissolve sodium salts by means of ion–dipole interactions between Na^+ ions and polymers. Thus, PU can be a promising polymer matrix for making gel polymer electrolytes with good compatibility with the liquid electrolyte, high mechanical strength, and elasticity.

[a] M.-S. Park, H.-S. Woo, J.-M. Heo, Prof. J.-M. Kim, Prof. D.-W. Kim
Department of Chemical Engineering
Hanyang University
Seoul 04763 (Republic of Korea)
E-mail: dongwonkim@hanyang.ac.kr

[b] R. Thangavel, Prof. Y.-S. Lee
Faculty of Applied Chemical Engineering
Chonnam National University
Gwangju 61186 (Republic of Korea)

Supporting Information and the ORCID identification number(s) for the author(s) of this article can be found under:
https://doi.org/10.1002/cssc.201901799.

Herein, we report gel polymer electrolytes based on a PU consisting of 4,4′-diphenylmethane diisocyanate-based hard segments and polyester-based soft segments for sodium-metal cells. Compatibility between PU and liquid electrolytes can have a vital influence on the ionic conductivity of the gel polymer electrolyte. In this respect, spectroscopic analysis including attenuated total reflectance (ATR) Fourier-transform (FT)IR and Raman spectroscopy was used to investigate the Na$^+$ ion–polymer interactions and the dissociation behavior of NaClO$_4$ in the gel polymer electrolyte. The optimized gel polymer electrolyte was then applied in a sodium cell with a sodium-metal anode and Na$_3$V$_2$(PO$_4$)$_3$ (NVP) cathode. For comparison, a conventional polyethylene (PE) separator soaked with liquid electrolyte was also applied to assemble sodium-metal cells. NVP was used as a cathode material owing to its Na superionic conductor (NASICON) structure, which can facilitate faster Na$^+$-ion diffusion in the electrode.[10] As a result, the sodium-metal cell employing the PU-based gel polymer electrolyte exhibited better cycling performance in terms of discharge capacity and rate capability than the cell assembled with liquid electrolyte. To the best of our knowledge, this is the first report on PU-based gel polymer electrolytes for sodium-metal cells. On the basis of our results, the PU-based gel polymer electrolyte is expected to serve as a reliable electrolyte system for sodium batteries with enhanced safety and good cycling stability.

Results and Discussion

Free-standing and flexible PU-based gel polymer electrolyte was prepared by solution casting and soaking in liquid electrolyte (Figure 1 a). Figure 1 b shows the secondary interactions occurring in the PU-based gel polymer electrolyte, which include hydrogen bonding and Na$^+$–carbonyl (ion–dipole) interactions. The detailed interactions are addressed in the subsequent discussion of the spectroscopic analyses. Biaxial stretching and tensile tests were conducted to evaluate the elasticity and mechanical properties of the gel polymer electrolyte. Gel polymer electrolyte was prepared with 30 wt% PU and 70 wt% liquid electrolyte. The liquid electrolyte used was 1.0 M NaClO$_4$ in ethylene carbonate (EC)/propylene carbonate (PC)/diethyl carbonate (DEC) (50:20:30 v/v/v). As shown in Figure 1 c, the PU-based gel polymer electrolyte could be biaxially stretched up to 180% without any mechanical damage. According to the stress–strain curve in Figure S1 in the Supporting Information, the tensile strength and elongation at break of the gel polymer electrolyte were 6.4 MPa and 610.1%, respectively.

The high mechanical stretchability and elongation at break can be ascribed to the phase separation between the hard and soft segments of the PU chains. Intermolecular hydrogen bonding between urethane groups results in domain association of hard blocks, which serve as physical anchor sites providing a restorative force when the film is stretched. When the gel polymer electrolyte is stretched, the polyester soft seg-
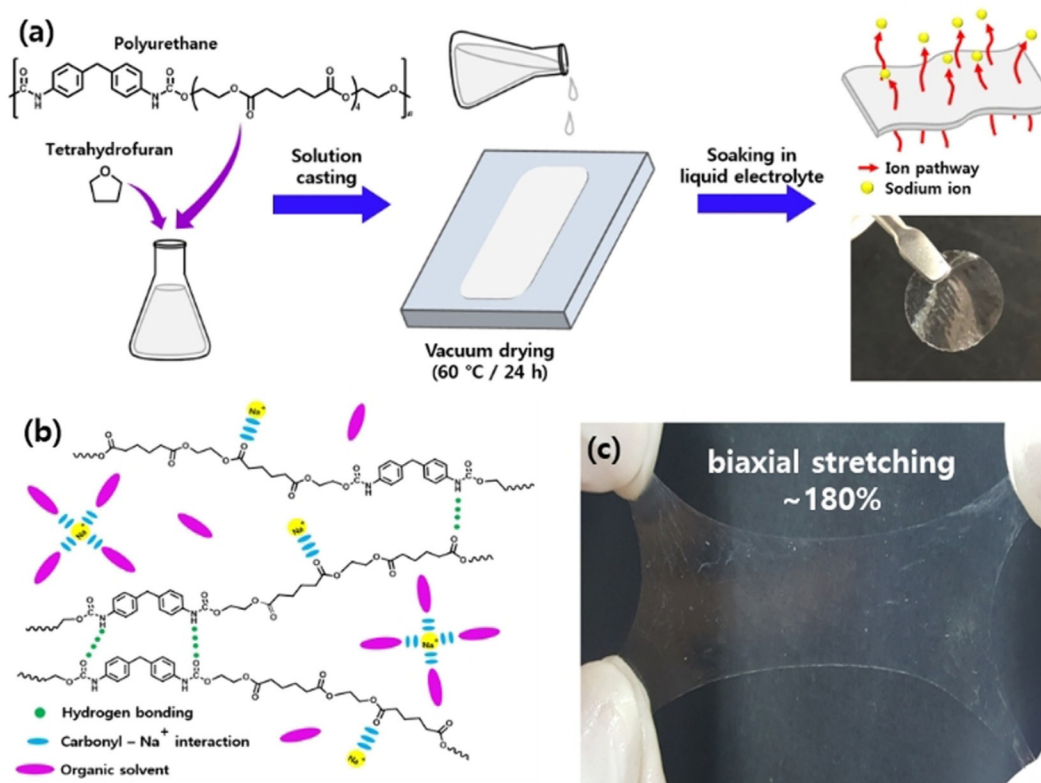

Figure 1. a) Schematic of the preparation of PU-based gel polymer electrolyte, b) Secondary interactions in the PU-based gel polymer electrolyte, and c) photograph of the gel polymer electrolyte under biaxial stretching.

ments elongate until tension is released, and this results in the high elasticity of the PU-based gel polymer electrolyte.

We investigated the effect of solvent composition on the ionic conductivity of the PU-based gel polymer electrolyte to obtain an optimized gel polymer electrolyte with high ionic conductivity. Cyclic carbonates (EC and PC) and a linear carbonate (DEC) were mixed and used as organic solvents in the liquid electrolytes to achieve a high degree of Na-salt dissociation and maintain low viscosity of the liquid electrolyte. The liquid electrolyte was composed of 1.0 M NaClO₄ in EC/PC/DEC (50:50−x:x v/v/v). The DEC content x was changed from 0 to 50 vol% in intervals of 10 vol%.

Figure 2 a, b shows the ionic conductivities of the liquid electrolytes and PU-based gel polymer electrolytes at ambient temperature as a function of DEC content. The ionic conductivity of the liquid electrolyte increased with increasing DEC content and reached a maximum value of 8.5 mS cm⁻¹ at 20 vol% DEC. The viscosity of the liquid electrolyte decreased with increasing DEC content, as shown in Figure S2 in the Supporting Information. These results demonstrate that EC/PC/DEC (50:30:20 v/v/v) is an optimum solvent composition that imparts a high degree of salt dissociation and low viscosity and results in the highest ionic conductivity of the liquid electrolyte. However, the gel polymer electrolyte exhibited the highest ionic conductivity of 1.5 mS cm⁻¹ at 30 vol% DEC, as shown in Figure 2 b. The optimum DEC content in the gel polymer electrolyte was higher than that in the liquid electrolyte. The ionic conductivity of the gel polymer electrolyte with EC/PC/DEC (50:0:50 v/v/v) was higher than that of the gel polymer electrolyte with EC/PC/DEC (50:50:0 v/v/v), whereas the liquid electrolyte showed the opposite tendency. These results suggest that the PU matrix is more compatible with DEC than PC, and therefore a higher electrolyte uptake of the PU film at the

higher DEC content results in the highest ionic conductivity at 30 vol% DEC. The contact angle of the liquid electrolyte on the PU film and electrolyte uptake of the PU film were measured to confirm the compatibility between the liquid electrolyte and PU (Figure 2 c and Table S1 in the Supporting Information). The contact angle on the PU film decreased from 65.5 to 33.0°, and the electrolyte uptake of the PU film increased from 106.6 to 179.1% with increasing DEC content. These results demonstrate that the gel polymer electrolyte prepared with 1.0 M NaClO₄ in EC/PC/DEC (50:20:30 rather than 50:30:20 v/v/v) has the highest ionic conductivity owing to the higher compatibility between liquid electrolyte and PU. To gain further insight into the ion conduction mechanism in the liquid electrolyte and gel polymer electrolyte, the temperature dependence of the ionic conductivity in the temperature range of −15 to 75 °C was investigated. The ionic conductivity of the electrolyte can be described by Arrhenius [Eq. (1)] or Vogel–Tammann–Fulcher (VTF) [Eq. (2)] behavior:[11]

$$\sigma = A \ \exp(-E_a/RT) \tag{1}$$

$$\sigma = AT^{-1/2} \ \exp[-E_a/R(T-T_0)] \tag{2}$$

in which σ is the ionic conductivity of the electrolyte, A is the pre-exponential factor, E_a the activation energy, R the gas constant, and T_0 the reference temperature, which is normally 10–50 K below the glass transition temperature. As shown in Figure S3 in the Supporting Information, the temperature dependence of the ionic conductivity in the liquid electrolyte follows the Arrhenius equation. For the gel polymer electrolyte, the plot of $\log \sigma$ versus $1/T$ is nonlinear and can be fitted by the VTF equation. These results suggest that the conductivity mechanism in the gel polymer electrolyte involves an ionic hopping motion coupled with segmental motion of the polymer chains.

ATR-FTIR analysis was performed to investigate the intermolecular interactions of polymer chains and ion–polymer interactions in the gel polymer electrolyte. Figures 3 a, b shows the ATR-FTIR spectra of the gel polymer electrolytes with optimum solvent composition (EC/PC/DEC 50:20:30 v/v/v) and different NaClO₄ concentrations in the wavenumber ranges of 3100–3500 and 1600–1900 cm⁻¹, respectively. For comparison, the ATR-FTIR spectra of liquid electrolytes with different NaClO₄ concentrations are shown in Figure S4 a in the Supporting Information. As shown in Figure 3 a, the intensity of the peak at 3330 cm⁻¹, corresponding to hydrogen-bonded N—H stretching, was maintained when the salt concentration increased. This result indicates that the high elasticity and tensile strength of the gel polymer electrolyte arose from the hydrogen bonds between urethane and carbonyl groups.[9c] In Figure 3 b, the peaks observed at 1700 and 1725 cm⁻¹ correspond to the free carbonyl stretching of urethane groups and ester groups in the PU, respectively.[9c, 12] The peaks around 1770–1800 cm⁻¹ and the peak at
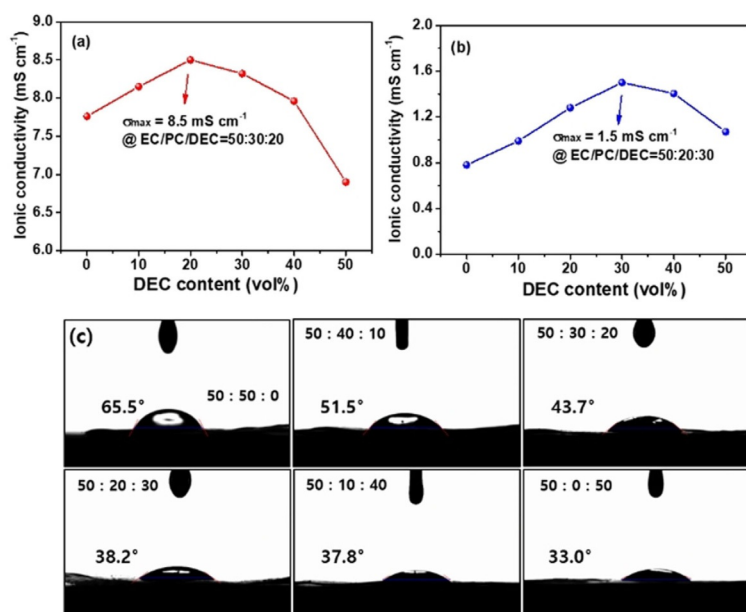

Figure 2. Ionic conductivities of a) liquid electrolytes and b) gel polymer electrolytes with various EC/PC/DEC volume ratios and c) contact angles of various liquid electrolytes with different solvent compositions on the PU film.
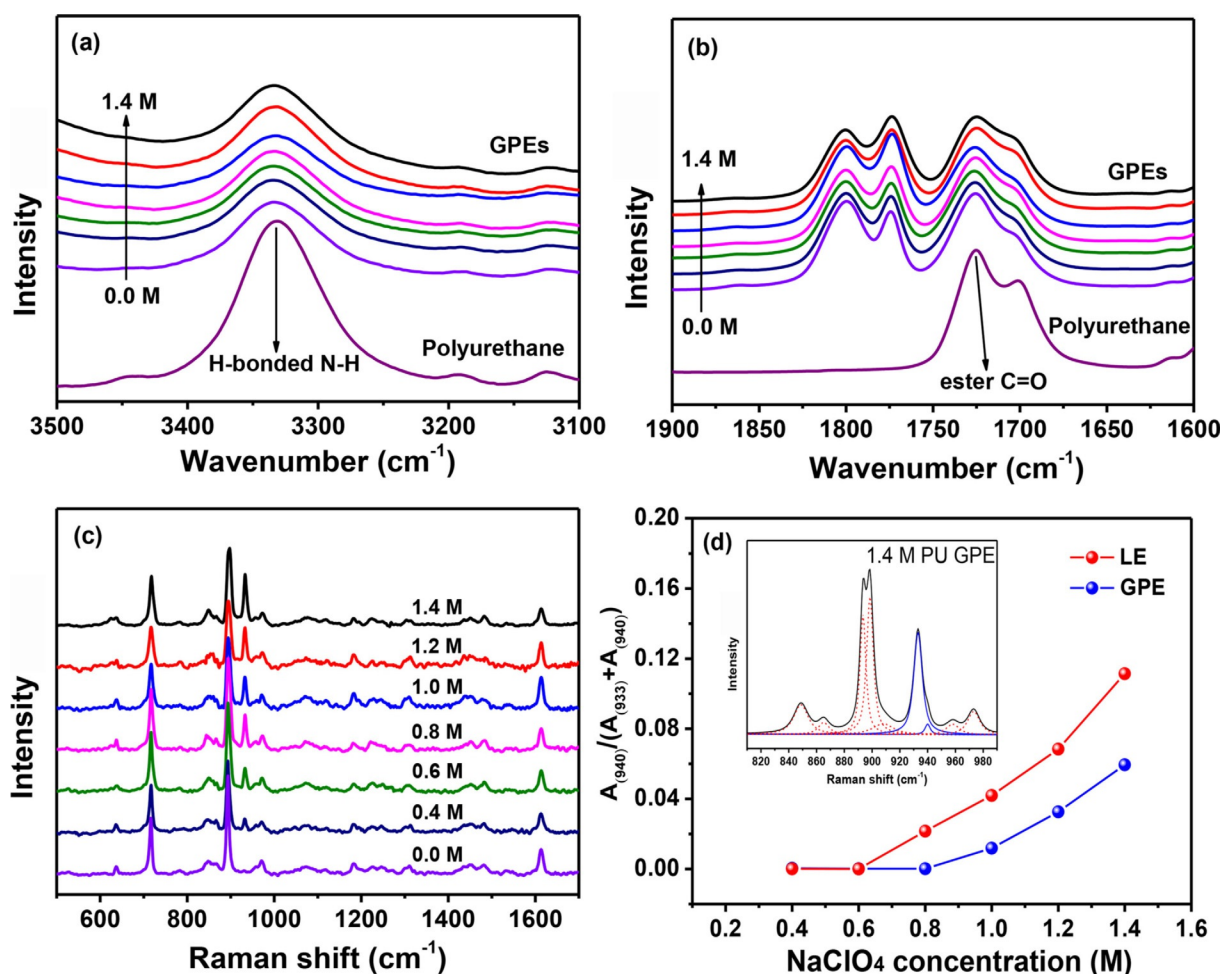
Figure 3. ATR-FTIR spectra of gel polymer electrolytes with different $NaClO_4$ concentrations in the wavenumber ranges of a) 3100–3500 cm^{-1} and b) 1600–1900 cm^{-1}, c) Raman spectra of the gel polymer electrolytes with different $NaClO_4$ concentrations, and d) relative fraction of contact ion-pairs of ClO_4^- anions as a function of $NaClO_4$ concentration in the liquid electrolytes and gel polymer electrolytes. The inset in d) shows a typical example of peak resolution of the ClO_4^- bands between 810 and 990 cm^{-1}. The volumetric ratio of EC/PC/DEC in liquid electrolyte and gel polymer electrolyte was 50:20:30.

1740 cm^{-1} in Figure S4a in the Supporting Information can be assigned to carbonyl stretching of EC and DEC, and the peak of PC at 1770 cm^{-1} is superimposed on the other organic-solvent peaks. For the gel polymer electrolyte, the intensity of the peak at 1725 cm^{-1} gradually decreased and the shoulder around 1710 cm^{-1} increased with increasing $NaClO_4$ concentration. The shoulder corresponds to the ester carbonyl groups of the PU coordinated with Na$^+$ ions, and the changes in the ATR-FTIR spectra of the gel polymer electrolyte indicate effective complexation of the Na salt by ester carbonyl groups of the PU in addition to coordination between the organic solvents and Na$^+$ ions.[12] This coordination can contribute to the high degree of $NaClO_4$ dissociation in the PU-based gel polymer electrolyte and result in high ionic conductivity because the polymer chains can additionally solvate the Na salt and transport Na$^+$ ions through local segmental motion of the flexible polymer chains.[13] Intensity changes related to the carbonyl stretching of the urethane groups could not be observed; that is, Na$^+$ ions are mainly coordinated by ester groups in the polymer chains.

Raman spectra of the gel polymer electrolytes and the liquid electrolytes are shown in Figure 3c and Figure S4b in the Supporting Information, respectively. All Raman spectra were background-corrected and normalized with respect to the band at 1480 cm^{-1}, which was unaffected by Na-salt concentration. To investigate the dissociation state of $NaClO_4$ in both electrolytes, we analyzed the vibrations of the free ClO_4^- anion with T_d symmetry. Although the free ClO_4^- anion has four Raman-active vibration modes, the symmetric stretching vibration $\nu_1(A_1)$ observed at 933 cm^{-1} was mainly characterized because of its high intensity and clarity.[14] As shown in Figure 3c and Figure S4b in the Supporting Information, the intensity of the band at 933 cm^{-1} increases with increasing $NaClO_4$ concentration. The shoulder at 940 cm^{-1}, corresponding to the contact ion–pairs of the ClO_4^- anion, appears at high $NaClO_4$ concentration. This phenomenon arises from band splitting of the ν_1 mode.[14b, 15] For a more detailed characterization of the dissociation of $NaClO_4$, the spectra of the gel polymer electrolytes and liquid electrolytes in the range of 810–990 cm^{-1} were resolved by using the Gaussian–Lorentzian function, and the relative fraction of contact ion-pairs of ClO_4^- anions was deter-

mined by calculating the value $\rho = A_{(940)}/(A_{(933)} + A_{(940)})$, in which $A_{(933)}$ and $A_{(940)}$ are the areas of the bands at 933 and 940 cm^{-1}, respectively. A typical example of such a resolution is shown in the inset of Figure 3d. The assignment of other bands in this region is summarized in Table S2 in the Supporting Information.[14b, 15] As shown in Figure 3d, the value of ρ is lower in the gel polymer electrolyte than in the liquid electrolyte. These results reveal that the additional interactions between Na$^+$ ions and polymer chains increase the degree of NaClO$_4$ dissociation in the PU-based gel polymer electrolytes.

Thermogravimetric analysis (TGA) was conducted to compare the evaporation behavior of volatile solvents in the gel polymer electrolyte and PE separator soaked with liquid electrolyte (Figure S5 in the Supporting Information). The PE separator soaked with liquid electrolyte showed a large weight loss of 85.9 wt% up to 200 °C owing to the evaporation of organic solvents. In comparison, the gel polymer electrolyte lost 66.2 wt% of its liquid electrolyte component. These results demonstrate that the gel polymer electrolyte has a better ability to retain organic solvents than the PE separator because of good compatibility with organic solvents as well as secondary interactions between the polymer chain and liquid electrolyte, which can suppress solvent loss.

The electrochemical stabilities of the gel polymer electrolyte and liquid electrolyte were examined by linear sweep voltammetry (LSV), and the results are shown in Figure 4. In the
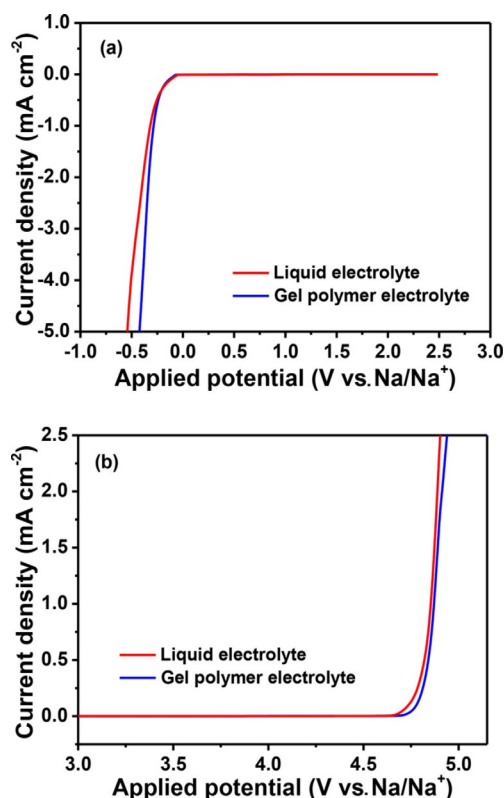

Figure 4. LSV of the liquid electrolyte and gel polymer electrolyte: a) cathodic scan and b) anodic scan (scan rate: 1 mV s^{-1}, temperature: 25 °C). The volumetric ratio of EC/PC/DEC in liquid electrolyte and gel polymer electrolyte was 50:20:30, and 5.0 wt% FEC was added to the mixed organic solvents.

cathodic scan, both electrolytes exhibited no reductive decomposition prior to 0 V vs. Na/Na$^+$. Both electrolytes showed a large reductive current around 0 V vs. Na/Na$^+$, which corresponds to sodium deposition (Na$^+$ + e → Na) on the electrode. With respect to anodic stability, the oxidative current started to rise around 4.7 V in both electrolytes owing to oxidative decomposition of the electrolytes. The gel polymer electrolyte exhibited slightly higher oxidative stability than the liquid electrolyte. Such suppressed oxidative decomposition of the gel polymer electrolyte can be attributed to the better trapping ability of the liquid electrolyte in the PU matrix. To evaluate the electrochemical stabilities of the gel polymer electrolyte and liquid electrolyte towards carbon-based electrodes, LSV was also performed with a working electrode prepared with Ketjenblack and poly(vinylidene fluoride). As shown in Figure S6 in the Supporting Information, the oxidative current started to gradually rise around 4.6 V, which indicates that the anodic stability is slightly decreased on the carbon electrode owing to the catalytic effect of carbon materials for electrolyte decomposition. In the case of the carbon electrodes, it was also confirmed that the electrochemical stability of the gel polymer electrolyte is superior to that of the liquid electrolyte.

The interfacial behavior between the sodium electrode and electrolytes was evaluated in a repeated plating/stripping cycling test of the symmetrical Na/electrolyte/Na cells at a current density of 0.5 mA cm^{-2} for 2 h. The DC polarization voltage profiles and magnified voltage profiles of the cells assembled with different electrolytes without fluoroethylene carbonate (FEC) during repeated plating/stripping cycling are shown in Figure 5a and Figure S7a in the Supporting Information, respectively. The cell employing the PE separator soaked with liquid electrolyte exhibited unstable DC polarization voltage profiles and a large overpotential. The unstable cycling behavior of the cell with liquid electrolyte arises from the irregular growth of sodium dendrites on the Na electrode and the continuous decomposition of liquid electrolyte at the Na metal with enlarged surface area. This is caused by uneven plating and stripping of sodium at the interface of the liquid electrolyte and Na electrode. The irreversible decomposition of the liquid electrolyte resulted in continuous accumulation of decomposition products and a large overpotential.[16] In contrast, the cell with gel polymer electrolyte showed more stable voltage profiles and a lower overpotential than the cell employing the liquid electrolyte. These results suggest that the gel polymer electrolyte can improve the cycling performance of Na-metal electrodes owing to the uniform sodium ion flux through the highly ion-conducting electrolyte. The migration behavior of Na$^+$ ions through the PU-based gel polymer electrolyte and the PE separator soaked with liquid electrolyte is schematically illustrated in Figure 5c. For the PE separator with liquid electrolyte, Na$^+$ ion flux is inclined to be concentrated at the interface between the separator pores and the Na electrode owing to the tortuous and porous structure of the PE separator, which causes irregular plating and stripping of sodium. In the case of the gel polymer electrolyte, sodium can be evenly plated and stripped because the favorable interfacial characteristics facilitate the charge-transfer reaction (Na$^+$ +
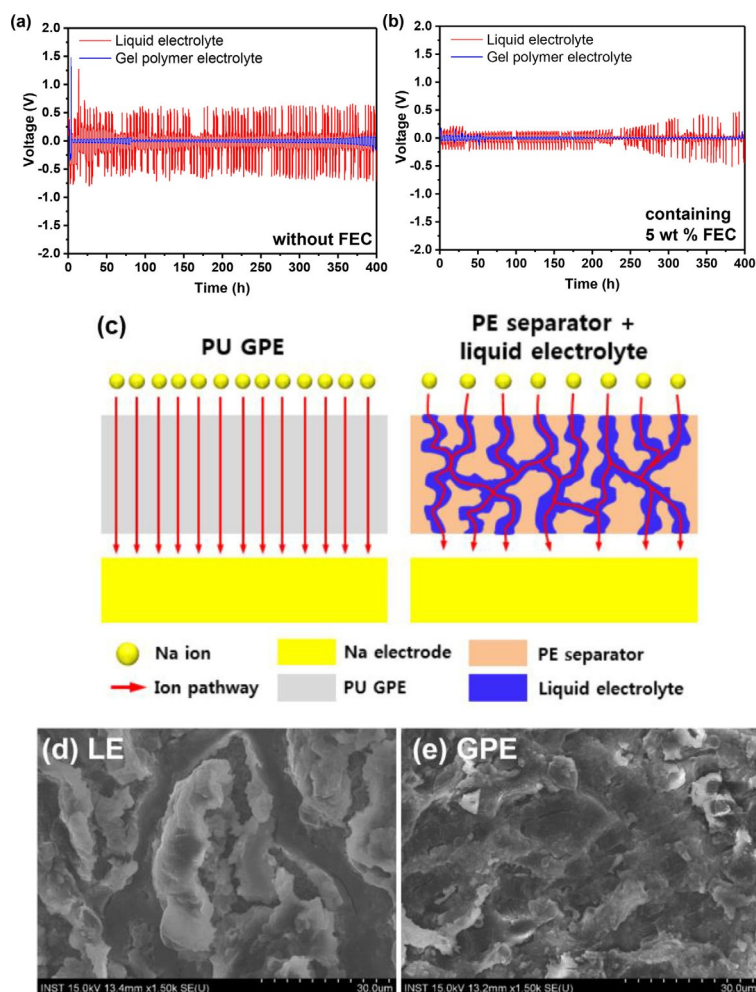
Figure 5. DC polarization voltage profiles of the symmetrical Na/electrolyte/Na cells with gel polymer electrolyte and liquid electrolyte (1.0 M $NaClO_4$ in EC/PC/DEC, 50:20:30 v/v/v) during the stripping/plating processes, which were obtained at a constant current density of 0.5 mA cm^{-2} for 2 h in the cutoff potential range of −2.0–2.0 V: a) without FEC and b) with 5 wt% FEC. c) Schematic of Na$^+$ ion transport through the gel polymer electrolyte and the PE separator soaked with liquid electrolyte during the electrochemical plating process. SEM images of sodium electrodes disassembled from symmetrical Na/electrolyte/Na cells with different electrolytes after cycles at 0.5 mA cm^{-2}: d) liquid electrolyte and e) gel polymer electrolyte.

e⇌Na) at the electrolyte/electrode interface. To investigate the effect of FEC on the electrochemical behavior of the symmetrical Na/electrolyte/Na cells, we conducted galvanostatic stripping/plating tests for cells assembled with electrolytes containing a small amount of FEC (5 wt%). As shown in Figure 5 b and Figure S7 b in the Supporting Information, the cells employing the electrolytes containing FEC showed more stable electrochemical performance than the cells employing electrolytes without FEC because FEC forms a stable solid electrolyte interphase (SEI) layer on the surface of the Na electrode.[17] As expected, the cell with gel polymer electrolyte showed more stable voltage profiles and a lower overpotential than the cell employing the liquid electrolyte owing to the uniform sodium ion flux through the highly ion-conducting electrolyte.

To further examine the electrochemical behavior of the Na electrode, SEM images were obtained after 20 cycles at

0.5 mA cm^{-2}. As shown in Figure 5 d, e, the sodium electrode cycled in the liquid electrolyte showed a highly uneven and rough surface with granule-like Na deposits. In contrast, the sodium electrode cycled with gel polymer electrolyte exhibited a relatively flat surface, indicating that sodium can be evenly plated and stripped owing to the uniform sodium-ion flux through the gel polymer electrolyte. The chemical composition of decomposition products formed on the sodium electrode was characterized by X-ray photoelectron spectroscopy (XPS), and the results are shown in Figure S8 in the Supporting Information. All XP spectra were normalized with respect to the Na Auger peak at 536.0 eV. The C 1s XP spectrum shows five peaks, which correspond to C−C species (285.0 eV), C−O species (286.8 eV), C=O species (288.0 eV), sodium alkyl carbonate (ROCO$_2$Na, 289.1 eV), and sodium carbonate (Na$_2$CO$_3$, 290.0 eV).[18] In the O 1s spectrum, four peaks corresponding to sodium oxide (Na$_2$O, 529.7 eV), sodium carbonate (Na$_2$CO$_3$, 531.6 eV), sodium hydroxide or C−O species (NaOH or C−O, 532.8 eV), and C=O species (534.1 eV) were observed.[18] These chemical components are formed by reductive decomposition of the liquid electrolyte. For the sodium electrode cycled in the gel polymer electrolyte, the lower peak intensities in the XP spectra compared with those in the XP spectra of the electrode cycled in the liquid electrolyte indicate suppressed decomposition of the electrolyte.

To further understand the cycling behavior of the Na/electrolyte/Na symmetric cells, their AC impedance was measured with stripping/plating cycling (Figure S9 in the Supporting Information). The depressed semicircle observed in the middle-to-low-frequency region arises from the interfacial resistances including the ionic resistance in the film formed on surface of the sodium electrode (R_f) and charge-transfer resistance (R_{ct}). The cell employing liquid electrolyte without FEC showed a gradual increase of interfacial resistance during cycling owing to the deleterious reaction of the liquid electrolyte with the sodium metal. In contrast, the interfacial resistance of the cell with gel polymer electrolyte without FEC initially increased and then stabilized. For the cells containing FEC, the interfacial resistances were lowered and rapidly stabilized, which can be ascribed to the formation of a stable SEI layer during initial cycles. The cell assembled with gel polymer electrolyte containing FEC exhibited quite stable and low interfacial resistance during cycling. These results confirm the stable cycling performance and lower overpotential of the Na/electrolyte/Na symmetric cell assembled with the gel polymer electrolyte containing FEC. The interfacial stability of gel polymer electrolyte in prolonged contact with the sodium electrode was also investigated from the time evolution of the AC impedance spectra of the Na/electrolyte/Na symmetric cells. As shown in Figure S10 in the Supporting Information, the cell with gel polymer electrolyte exhibited

better interfacial stability than the cell with liquid electrolyte. This is because the use of gel polymer electrolyte allows the liquid electrolyte to be effectively encapsulated in the PU matrix and good interfacial contact between electrolyte and electrodes to be maintained.

The sodium transference number t^+ in the liquid electrolyte and gel polymer electrolyte was measured by using a combination of AC impedance and DC polarization measurements, as proposed by Evans et al.[19] The AC impedance of the Na/electrolyte/Na cell was measured to determine the initial interfacial resistance. A 10 mV DC potential was then applied to the cell, and the current was monitored with time until a steady-state current was attained. The steady-state interfacial resistance of the cell was determined by AC impedance measurement. From the data given in Figure S11 a, b in the Supporting Information, the sodium transference number in the gel polymer electrolyte was calculated to be 0.22. In comparison, the value of t^+ in the liquid electrolyte was measured to be 0.25. The smaller t^+ value in the gel polymer electrolyte is owing to the fact that the Na$^+$ ions are strongly coordinated by the polar polymer chains through ion–dipole interactions.

Cycling performance of sodium-metal cells assembled with gel polymer electrolyte and liquid electrolyte was evaluated at a constant current rate of 0.25 C. A small amount of FEC (5 wt%) was added to the electrolytes as an SEI-forming agent. The cell was composed of Na metal as anode and carbon-coated NVP as cathode. Figure 6a shows the charge and discharge curves of the sodium-metal cell assembled with gel polymer electrolyte as a function of cycle number at 25 °C. The voltage profiles of the cell showed a plateau at approximately 3.4 V vs. Na/Na$^+$, corresponding to the redox potential of the NVP electrode. The cell showed very stable cycling behavior during repeated cycling owing to the highly reversible phase transformation in the carbon-coated NVP electrode.

Figure 6b shows the cycling performance of the sodium-metal cells assembled with liquid electrolyte and gel polymer electrolyte. The cell employing the gel polymer electrolyte initially delivered a high discharge capacity of 111.7 mAh g^{-1} based on the NVP cathode material, and the cell with liquid electrolyte had an initial discharge capacity of 107.9 mAh g^{-1}. The higher initial discharge capacity of the cell with gel polymer electrolyte comes from the higher ionic conductivity of the gel polymer electrolyte. The ionic conductivity of the PE separator filled with liquid electrolyte (0.5 mS cm^{-1}) is lower than that of the gel polymer electrolyte (1.5 mS cm^{-1}) owing to the combination of tortuosity and porosity of the separator.
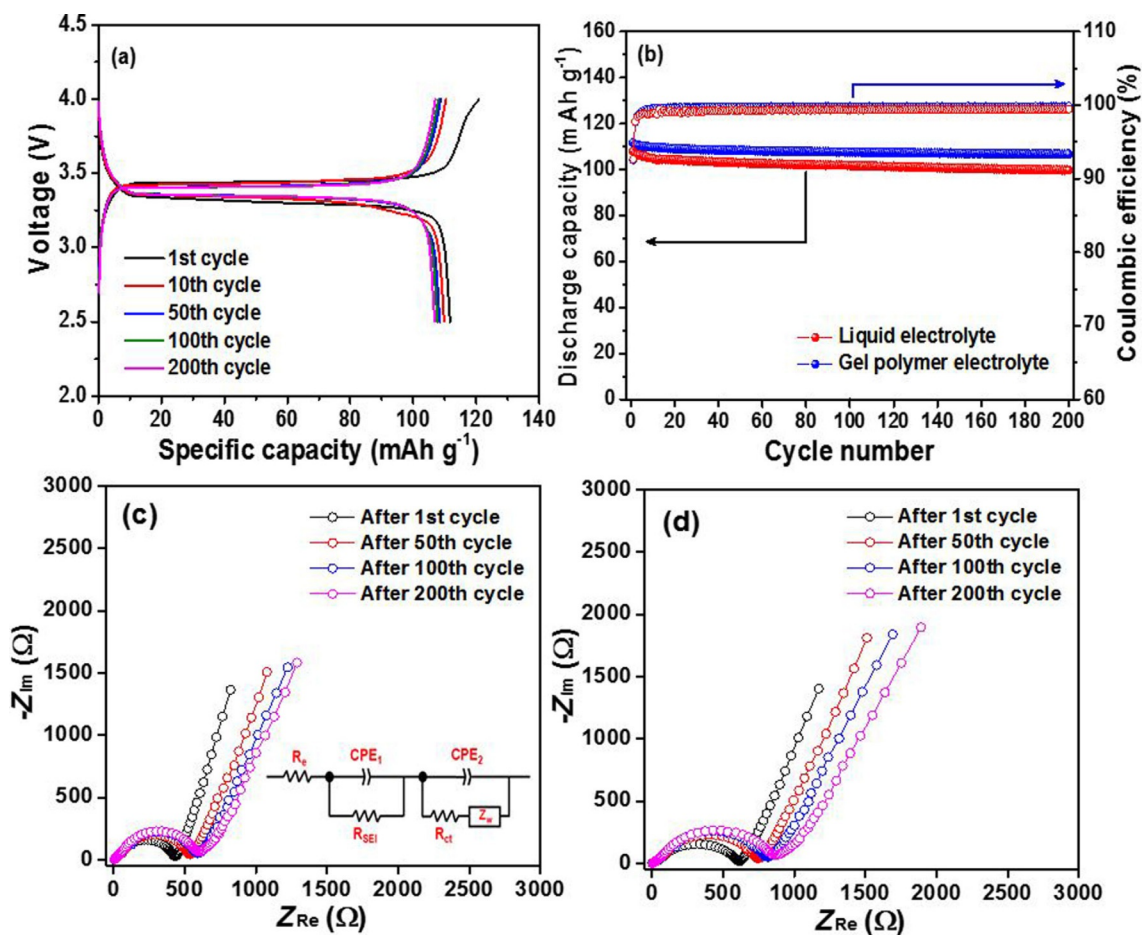

Figure 6. a) Charge and discharge curves of the Na/NVP cell with gel polymer electrolyte at 0.25 C rate. b) Discharge capacities and coulombic efficiencies of the Na/NVP cells assembled with different electrolytes at 0.25 C and 25 °C. AC impedance spectra of the Na/NVP cells assembled with c) gel polymer electrolyte and d) liquid electrolyte. The organic solvent was EC/PC/DEC (50:20:30 v/v/v) containing 5 wt% FEC.

The elastic and adhesive nature of the gel polymer electrolyte can also promote adhesion to the electrodes, which enhances the interfacial charge transport between the electrodes and gel polymer electrolyte. As discussed above, the PU in the gel polymer electrolyte effectively holds the organic solvents, which are highly reactive toward sodium metal, suppresses their leakage, and thus results in good cycling stability. The cell with gel polymer electrolyte maintained high and stable coulombic efficiencies over 99.5% throughout cycling after the initial cycles. The cycling performance of the Na/NVP cell with the best liquid electrolyte [1.0 M NaClO$_4$ in EC/PC/DEC (50:30:20 v/v/v) + 5 wt% FEC] was also evaluated, and the results are compared in Figure S12 in the Supporting Information. The cycling performance of the cell with 50:30:20 composition was almost the same as that of the cell with 50:20:30 composition with respect to cycling stability and rate capability. This is because the ionic conductivities of two electrolytes differ only slightly (8.5 mS cm^{-1} for 50:30:20 and 8.3 mS cm^{-1} for 50:20:30). The AC impedance of the cells with liquid electrolyte and gel polymer electrolyte was measured with cycling, and the resulting spectra are shown in Figure 6 c, d, respectively. An equivalent circuit to fit the experimental data is given in the inset of Figure 6 c. For the cell with gel polymer electrolyte, the interfacial resistance initially increased and stabilized in the

subsequent cycles. In contrast, the cell with liquid electrolyte exhibited higher interfacial resistance than that with gel polymer electrolyte, and the interfacial resistance continuously increased with cycling. These results demonstrate that the use of gel polymer electrolyte is more effective for achieving good cycling stability of the sodium-metal cell.

The rate capability of the Na/NVP cells with gel polymer electrolyte and liquid electrolyte was examined by increasing the current rate from 0.1 to 5.0 C. Figure 7 a, b shows the voltage profiles of the cells assembled with gel polymer electrolyte and liquid electrolyte at different current rates, and Figure 7 c compares the rate capabilities of the cells with different electrolytes. It is noteworthy that the cell employing gel polymer electrolyte exhibited lower overpotential and higher discharge capacities at all the current rates investigated compared with the cell with liquid electrolyte. A high discharge capacity of 96.7 mAh g^{-1} was obtained at 5.0 C in the cell with gel polymer electrolyte, whereas the liquid-electrolyte-based cell delivered a lower discharge capacity of 52.3 mAh g^{-1} at the same C rate. Such a superior rate capability of the cell with gel polymer electrolyte results from both the higher ionic conductivity of the gel polymer electrolyte compared with the PE separator soaked with liquid electrolyte and favorable interfacial characteristics, which allow a fast charge-transfer reaction. Interest-
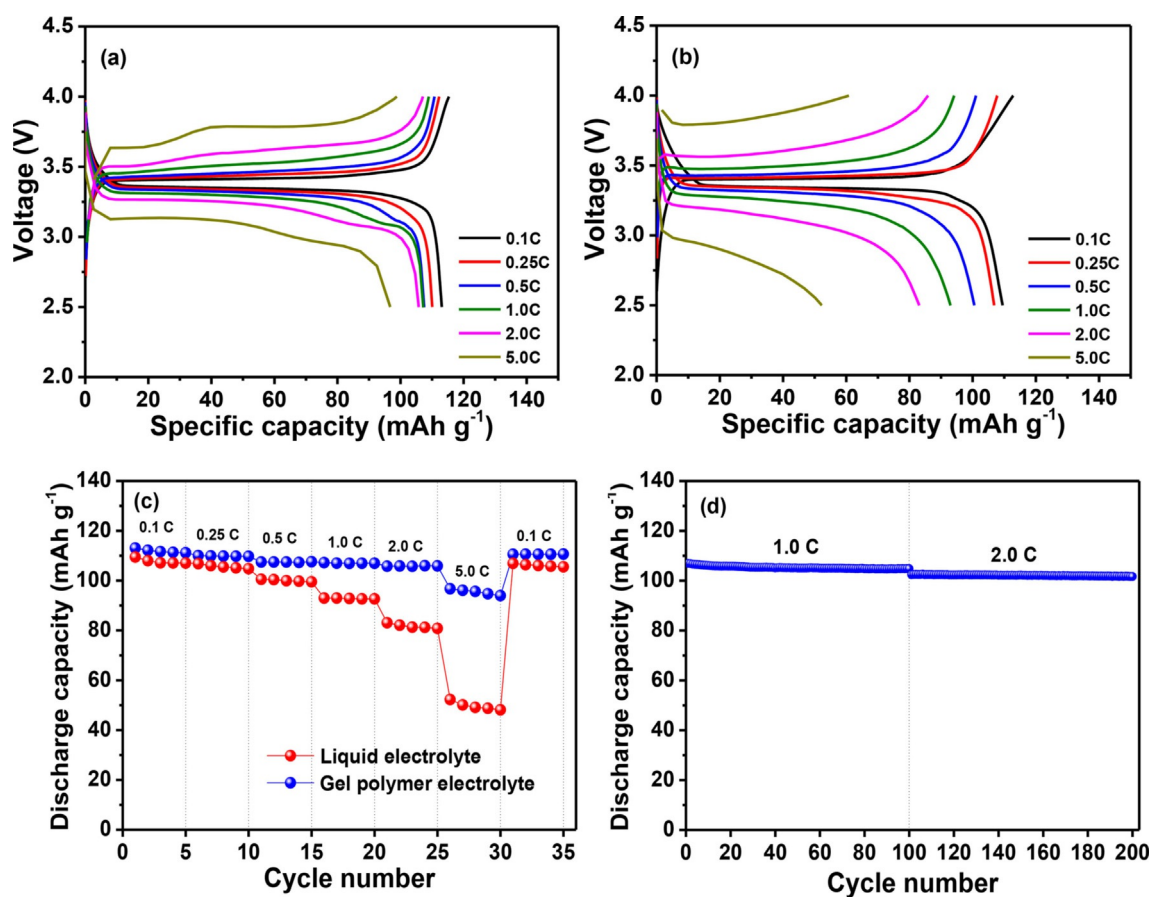

Figure 7. Charge and discharge curves of the Na/NVP cells with a) gel polymer electrolyte and b) liquid electrolyte at various C rates. (c) Discharge capacities of the Na/NVP cells employing different electrolytes at different C rates. The C rate was increased from 0.1 to 5.0 C after every five cycles. d) Cycling performance of the Na/NVP cell with gel polymer electrolyte at 1.0 and 2.0 C. The organic solvent was EC/PC/DEC (50:20:30 v/v/v) containing 5 wt% FEC.

ingly, we could observe a step in the voltage profile of the cell with gel polymer electrolyte at high C rates. It can be attributed to structural rearrangement of the NVP cathode at high current rates.[20] To further investigate the electrochemical behavior of the Na/NVP cells, cyclic voltammetry (CV) was conducted (Figure S13 in the Supporting Information). The cell with gel polymer electrolyte showed higher peak current and lower potential difference between anodic peak and cathodic peak. This result indicates facile electrochemical reaction kinetics and low overpotential in the cell with gel polymer electrolyte, which are consistent with superior rate capability of the Na/NVP cell employing gel polymer electrolyte. The cycling stability of the Na/NVP cell with gel polymer electrolyte was further investigated at higher current rates of 1.0 and 2.0 C for 100 cycles. As shown in Figure 7d, the cell exhibited high discharge capacities and stable cycling behavior even at high current rates. From these results, it is expected that PU-based gel polymer can be a promising electrolyte for sodium metal batteries with good cycling stability and enhanced safety.

Conclusion

A thermoplastic polyurethane (PU)-based gel polymer electrolyte with high elasticity and high ionic conductivity was prepared and characterized for sodium-battery applications. The PU matrix was more compatible with diethyl carbonate than propylene carbonate in liquid electrolyte. The spectroscopic analyses revealed that Na^+ ions were additionally coordinated by polar polymer chains, and such additional ion–polymer interactions could enhance the dissociation of sodium salt. The gel polymer electrolyte showed more favorable interfacial characteristics toward Na metal electrodes than a polyethylene separator soaked with liquid electrolyte owing to the high ionic conductivity and uniform sodium-ion flux through the gel polymer electrolyte. The Na/$Na_3V_2(PO_4)_3$ (NVP) cell with PU-based gel polymer electrolyte exhibited a high initial discharge capacity of 111.7 mA h g^{-1} with good capacity retention and better rate capability than the cell employing liquid electrolyte. Our results demonstrate that the PU-based gel polymer electrolyte can be used as a promising electrolyte material for sodium-based energy-storage devices.

Experimental Section

Preparation of gel polymer electrolyte

The electrolyte was prepared in a glovebox filled with high-purity argon gas. $NaClO_4$ (anhydrous, 99.5%, Alfa Aesar) was used after vacuum drying at 120 °C for 24 h. DEC (anhydrous, ≥99.0%, Sigma–Aldrich), EC (anhydrous, 99.0%, Sigma–Aldrich), and PC (anhydrous, 99.7%, Sigma–Aldrich) were used as organic solvents. A ternary solvent mixture was prepared by mixing EC, PC, and DEC with a volumetric ratio of 50:50−x:x. The liquid electrolytes were dried over molecular sieves to reduce water content. The water content in the electrolytes was less than 25 ppm, as measured by Karl-Fischer titration. The thermoplastic PU (K-480A) was kindly supplied by Kolon Industries, Inc. PU (10 g) was dissolved in THF (anhydrous, >99.5%, TCI, 90 g), and the solution was stirred for

24 h. The polymer solution was then cast with a doctor blade onto a glass plate and left to evaporate the THF solvent at ambient temperature. It was subsequently dried under vacuum at 60 °C for 24 h. After vacuum drying, the resulting film was soaked in liquid electrolyte to obtain the gel polymer electrolyte with a thickness of 60–70 μm.

Electrode preparation and cell assembly

Carbon-coated NVP was synthesized by the sol–gel method, as described in our previous work.[10a] The NVP electrode was prepared by coating an N-methyl-2-pyrrolidone-based slurry containing 80 wt% NVP, 10 wt% Ketjenblack, and 10 wt% poly(vinylidene fluoride) onto an aluminum foil. The active mass loading on the electrode was approximately 5.0 mg cm^{-2}. Sodium metal (Sigma–Aldrich) was used as the anode. A sodium-metal cell was assembled by sandwiching the gel polymer electrolyte between the sodium foil and NVP electrode in a CR2032-type coin cell. A liquid-electrolyte-based cell was also prepared by using a PE separator (Hipore SV718, Asahi Kasei Chemicals) soaked with 1.0 M $NaClO_4$ in EC/PC/DEC (50:20:30 v/v/v) containing 5.0 wt% FEC (battery grade, PANAX ETEC Co. Ltd.). All cells were assembled in a glovebox filled with high-purity argon gas.

Characterization and measurements

The ionic conductivity and viscosity of the liquid electrolytes were measured by using a Cond 3210 conductivity meter (WTW GmbH, Germany) and a viscometer (RheoSense, microVISC, USA), respectively, at ambient temperature. The ionic conductivity of the gel polymer electrolyte was determined from AC impedance measurements by using an impedance analyzer (Zahner Electrik, IM6) over the frequency range from 10 Hz to 1 MHz with an amplitude of 20 mV at different temperatures. The gel polymer electrolyte was sandwiched between two stainless-steel blocking electrodes for the conductivity measurements. Before the impedance measurements, each sample was stored at the required temperature for at least 1 h. A representative AC impedance spectrum of the gel polymer electrolyte is shown in Figure S14 in the Supporting Information. The high-frequency intercept on the real axis corresponds to the bulk resistance R_b of the gel polymer electrolyte. Ionic conductivity could be calculated by using $\sigma = t/(R_b A)$, in which t and A are the thickness and area of the electrolyte film, respectively. The stress–strain behavior of the gel polymer electrolyte was obtained by using a universal testing machine (Instron 5966) at a stretching speed of 2 mm min^{-1}. The sample dimensions were 20×40 mm (width×length). Uptake of liquid electrolyte was measured by immersing the PU film in the liquid electrolyte for 3 h and then measuring its weight. The excess liquid electrolyte on its surface was removed by wiping with tissue paper. The electrolyte uptake was then calculated as uptake [%] = $(W−W_o)/W_o \times 100$, in which W_o is the weight of the dry PU film and W the weight of the gel polymer electrolyte obtained after soaking in the liquid electrolyte. The contact angle of the liquid electrolyte on a PU film was measured within 3 s to avoid any contamination. To evaluate the electrochemical stability of the electrolyte, LSV was conducted on a platinum working electrode with sodium metal as the reference and counter electrodes at a scan rate of 1.0 mV s^{-1} at 25 °C. ATR-FTIR spectra were recorded with a Nicolet iS50 spectrometer in the range of 400–4000 cm^{-1}. Raman spectra were recorded with a LabRAM HR Evolution Raman spectrometer (Horiba Scientific, 785 nm laser source). TGA was performed by using a thermal analyzer (SDT Q600, TA Instrument) in the temperature range from 30

to 200 °C at a heating rate of 5 °C min^{-1}. Galvanostatic stripping and plating in the symmetric Na/electrolyte/Na cell was conducted in the potential range of -2.0–2.0 V at a constant current density of 0.5 mA cm^{-2} for 2 h. The morphological analysis was conducted by SEM (JEOL JSM 6701F). The chemical products formed on the Na-metal electrode were investigated by XPS (VG Multilab ESCA system, 220i). The sodium ion transference number t^+ in the electrolyte was measured in the symmetrical Na/electrolyte/Na cell by using a combination of AC impedance and DC polarization measurements at 25 °C.[19] Galvanostatic charge and discharge cycling tests of the Na/NVP cells were performed in the voltage range 2.5–4.0 V by using a battery cycler (WBCS 3000, Wonatech) at 25 °C. CV was conducted with a CH instrument (CHI 600D) in the potential range of 2.5–4.0 V with a scan rate of 0.1 mV s^{-1} at 25 °C. AC impedance analysis of the cells was performed with an impedance analyzer over the frequency range of 5 mHz to 100 kHz with an amplitude of 5 mV.

Acknowledgements

Conflict of interest

The authors declare no conflict of interest.

[1] a) J. M. Tarascon, M. Armand, *Nature* **2001**, *414*, 359–367; b) M. Armand, J. M. Tarascon, *Nature* **2008**, *451*, 652–657; c) V. Etacheri, R. Marom, R. Elazari, G. Salitra, D. Aurbach, *Energy Environ. Sci.* **2011**, *4*, 3243–3262; d) B. Dunn, H. Kamath, J. M. Tarascon, *Science* **2011**, *334*, 928–935.

[2] a) H. Kawamoto, W. Tamaki, *Sci. Technol. Trends, Quart. Rev.* **2011**, *39*, 51; b) N. Yabuuchi, K. Kubota, M. Dahbi, S. Komaba, *Chem. Rev.* **2014**, *114*, 11636–11682; c) M. D. Slater, D. Kim, E. Lee, C. S. Johnson, *Adv. Funct. Mater.* **2013**, *23*, 947–958.

[3] a) S. Y. Hong, Y. Kim, Y. Park, A. Choi, N.-S. Choi, K. T. Lee, *Energy Environ. Sci.* **2013**, *6*, 2067–2081; b) J. Y. Hwang, S. T. Myung, Y. K. Sun, *Chem. Soc. Rev.* **2017**, *46*, 3529–3614.

[4] a) M. Dahbi, N. Yabuuchi, M. Fukunishi, K. Kubota, K. Chihara, K. Tokiwa, X.-f. Yu, H. Ushiyama, K. Yamashita, J.-Y. Son, Y.-T. Cui, H. Oji, S. Komaba, *Chem. Mater.* **2016**, *28*, 1625–1635; b) S. Komaba, W. Murata, T. Ishikawa, N. Yabuuchi, T. Ozeki, T. Nakayama, A. Ogata, K. Gotoh, K. Fujiwara, *Adv. Funct. Mater.* **2011**, *21*, 3859–3867; c) E. de la Llave, V. Borgel, K. J. Park, J. Y. Hwang, Y. K. Sun, P. Hartmann, F. F. Chesneau, D. Aurbach, *ACS Appl. Mater. Interfaces* **2016**, *8*, 1867–1875; d) X. Rui, W. Sun, C. Wu, Y. Yu, Q. Yan, *Adv. Mater.* **2015**, *27*, 6670–6676.

[5] a) H. Che, S. Chen, Y. Xie, H. Wang, K. Amine, X.-Z. Liao, Z.-F. Ma, *Energy Environ. Sci.* **2017**, *10*, 1075–1101; b) D. Zhou, R. Liu, J. Zhang, X. Qi, Y.-B. He, B. Li, Q.-H. Yang, Y.-S. Hu, F. Kang, *Nano Energy* **2017**, *33*, 45–54.

[6] a) Z. Xue, D. He, X. Xie, *J. Mater. Chem. A* **2015**, *3*, 19218–19253; b) X. Qi, Q. Ma, L. Liu, Y.-S. Hu, H. Li, Z. Zhou, X. Huang, L. Chen, *ChemElectroChem* **2016**, *3*, 1741–1745.

[7] a) W. K. Shin, J. Cho, A. G. Kannan, Y.-S. Lee, D.-W. Kim, *Sci. Rep.* **2016**, *6*, 26332; b) Y.-S. Lee, J. H. Lee, J.-A. Choi, W. Y. Yoon, D.-W. Kim, *Adv. Funct. Mater.* **2013**, *23*, 1019–1027; c) H. Gao, W. Zhou, K. Park, J. B. Goodenough, *Adv. Energy Mater.* **2016**, *6*, 1600467.

[8] a) J. I. Kim, Y. Choi, K. Y. Chung, J. H. Park, *Adv. Funct. Mater.* **2017**, *27*, 1701768; b) F. Bella, F. Colò, J. R. Nair, C. Gerbaldi, *ChemSusChem* **2015**, *8*, 3668–3676; c) Y. Zhu, Y. Yang, L. Fu, Y. Wu, *Electrochim. Acta* **2017**, *224*, 405–411.

[9] a) J. W. C. Van Bogart, P. E. Gibson, S. L. Cooper, *J. Polym. Sci. Polym. Phys. Ed.* **1983**, *21*, 65–95; b) J. Bao, G. Shi, C. Tao, C. Wang, C. Zhu, L. Cheng, G. Qian, C. Chen, *J. Power Sources* **2018**, *389*, 84–92; c) T.-C. Wen, S.-S. Luo, C.-H. Yang, *Polymer* **2000**, *41*, 6755–6764.

[10] a) R. Thangavel, K. Kaliyappan, K. Kang, X. Sun, Y.-S. Lee, *Adv. Energy Mater.* **2016**, *6*, 1502199; b) Y. H. Jung, C. H. Lim, D. K. Kim, *J. Mater. Chem. A* **2013**, *1*, 11350–11354.

[11] E. Quartarone, P. Mustarelli, *Chem. Soc. Rev.* **2011**, *40*, 2525–2540.

[12] M.-S. Park, Y.-C. Jung, D.-W. Kim, *Solid State Ionics* **2018**, *315*, 65–70.

[13] C. S. Kim, S. M. Oh, *Electrochim. Acta* **2000**, *45*, 2101–2109.

[14] a) N. Boaretto, A. Bittner, C. Brinkmann, B. E. Olsowski, J. Schulz, M. Seyfried, K. Vezzu, M. Popall, V. Di Noto, *Chem. Mater.* **2014**, *26*, 6339–6350; b) Z. Wang, B. Huang, R. Xue, L. Chen, X. Huang, *J. Electrochem. Soc.* **1998**, *145*, 3346–3350.

[15] V. Di Noto, V. Zago, S. Biscazzo, M. Vittadello, *Electrochim. Acta* **2003**, *48*, 541–554.

[16] D. Aurbach, E. Zinigard, Y. Cohen, H. Teller, *Solid State Ionics* **2002**, *148*, 405–416.

[17] Y. Lee, J. Lee, H. Kim, K. Kang, N.-S. Choi, *J. Power Sources* **2016**, *320*, 49–58.

[18] Y.-J. Kim, H. Lee, H. Noh, J. Lee, S. Kim, M.-H. Ryou, Y. M. Lee, H.-T. Kim, *ACS Appl. Mater. Interfaces* **2017**, *9*, 6000–6006.

[19] J. Evans, C. A. Vincent, P. G. Bruce, *Polymer* **1987**, *28*, 2324–2328.

[20] a) K. Saravanan, C. W. Mason, A. Rudola, K. H. Wong, P. Balaya, *Adv. Energy Mater.* **2013**, *3*, 444–450; b) W. Song, X. Ji, Z. Wu, Y. Zhu, Y. Yang, J. Chen, M. Jing, F. Li, C. E. Banks, *J. Mater. Chem. A* **2014**, *2*, 5358–5362.